ASBMB
JOURNAL OF LIPID RESEARCH

Lipid body formation during maturation of human mast cells

Andrea Dichlberger,* Stefanie Schlager,* Jani Lappalainen,* Reijo Käkelä,† Katarina Hattula,§ Sarah J. Butcher,§ Wolfgang J. Schneider,[1], and Petri T. Kovanen[1],***

Wihuri Research Institute,* 00140 Helsinki, Finland; Department of Biosciences† and Institute of Biotechnology,§ FIN-00014 University of Helsinki, Finland; and Department of Medical Biochemistry,** Medical University Vienna, 1030 Vienna, Austria

Abstract Lipid droplets, also called lipid bodies (LB) in inflammatory cells, are important cytoplasmic organelles. However, little is known about the molecular characteristics and functions of LBs in human mast cells (MC). Here, we have analyzed the genesis and components of LBs during differentiation of human peripheral blood-derived CD34$^+$ progenitors into connective tissue-type MCs. In our serum-free culture system, the maturing MCs, derived from 18 different donors, invariably developed triacylglycerol (TG)-rich LBs. Not known heretofore, the MCs transcribe the genes for perilipins (PLIN)1-4, but not PLIN5, and PLIN2 and PLIN3 display different degrees of LB association. Upon MC activation and ensuing degranulation, the LBs were not cosecreted with the cytoplasmic secretory granules. Exogenous arachidonic acid (AA) enhanced LB genesis in Triacsin C-sensitive fashion, and it was found to be preferentially incorporated into the TGs of LBs. The large TG-associated pool of AA in LBs likely is a major precursor for eicosanoid production by MCs. In summary, we demonstrate that cultured human MCs derived from CD34$^+$ progenitors in peripheral blood provide a new tool to study regulatory mechanisms involving LB functions, with particular emphasis on AA metabolism, eicosanoid biosynthesis, and subsequent release of proinflammatory lipid mediators from these cells.—Dichlberger, A., S. Schlager, J. Lappalainen, R. Käkelä, K. Hattula, S. J. Butcher, W. J. Schneider, and P. T. Kovanen. **Lipid body formation during maturation of human mast cells. *J. Lipid Res.* 2011.** 52: **2198–2208.**

Supplementary key words arachidonic acid • eicosanoids • fatty acid • inflammation • perilipin • secretory granules • triacylglycerol

Cytosolic lipid droplets are highly dynamic organelles, which depending on the metabolic state of the organism, can be found in almost any type of cell (1). Currently, the role of lipid droplets in the pathophysiology of obesity-dependent metabolic diseases involving insulin resistance is studied intensively (2). Lipid droplets are also present in various types of inflammatory cells (3–6), where they are usually called lipid bodies (LB) and participate in cell signaling and in the generation of biologically active lipid mediators evoked by inflammatory and infectious conditions (7–11).

Lipid bodies consist of a neutral lipid core that is surrounded by a monolayer of amphipathic lipids (phospholipids and unesterified cholesterol) and by proteins involved in the formation and trafficking of the LBs and in the turnover of their lipids. Depending on the type and metabolic state of a cell, the protein and lipid compositions of the LBs may vary considerably, reflecting active metabolism of their lipid components (12). The main proteins known to regulate the metabolism of the LB lipids are the members of the PAT protein family, mostly studied in adipocytes. This family includes five perilipins: perilipin 1 (PLIN1; formerly perilipin), perilipin 2 (PLIN2; formerly adipose differentiation-related protein), perilipin 3 (PLIN3; formerly tail-interacting protein of 47 kDa), perilipin 4 (PLIN4; formerly S3-12), and perilipin 5 (PLIN5; formerly lipid storage droplet protein 5) (13). PLIN1 regulates the lipolytic activity of adipose triglyceride lipase (ATGL) during triacylglycerol (TG) mobilization via interacting with its coactivating factor, the comparative gene identification 58 (CGI-58) (14), whereas overexpression

This work was supported by the Academy of Finland (Centre of Excellence Programme in Virus Research, 2006-2011; 129684 to S.J.B. and Academy researcher fellowship 129148 to R.K.) and by the Sigrid Juselius Foundation (S.J.B.). A.D. was supported by an Erwin Schrödinger Fellowship (J2994-B20) of the Austrian Science Fund (FWF). W.J.S. is a senior visiting researcher of the Sigrid Juselius Foundation, Helsinki, Finland. The Wihuri Research Institute is maintained by the Jenny and Antti Wihuri Foundation.

Manuscript received 16 August 2011 and in revised form 9 September 2011.

Published, JLR Papers in Press, October 4, 2011
DOI 10.1194/jlr.M019737

Abbreviations: AA, arachidonic acid; ACSL, long-chain acyl-CoA synthetase; ATGL, adipose triglyceride lipase; CE, cholesterol ester; CGI-58, comparative-gene-identification 58; LB, lipid body; LD, lipid droplet; LPS, lipopolysaccharide; lyso-PC, lyso-phosphatidylcholine; MC, mast cell; OA, oleic acid; PC, phosphatidylcholine; PGD2, prostaglandin D2; PLIN, perilipin; SA, stearic acid; SCF, stem cell factor; TC-MC, tryptase and chymase-containing mast cell; TEM, transmission electron microscopy; TG, triacylglycerol; TIP47, tail-interacting protein of 47 kDa; T-MC, tryptase-containing mast cell; UC, unesterified cholesterol.

[1]To whom correspondence should be addressed.
e-mail: petri.kovanen@wri.fi (P.T.K); wolfgang.schneider@meduniwien.ac.at (W.J.S.)

of PLIN2 enhances the accumulation of lipids in newly formed LBs by inhibiting β-oxidation (15). PLIN3 has been shown to enhance TG accumulation by binding and transporting free fatty acids from cytoplasm to LBs (16). PLIN4 is predominantly expressed in fat-storing adipose tissue, and similar to PLIN3, it is translocated from cytoplasmic compartments to LBs upon incubation with fatty acids (17). Finally, PLIN5, which is solely expressed in fatty acid-oxidizing tissues, has been shown to interact with CGI-58 or ATGL, thus leading to either an increase or decrease in lipolysis, respectively (18).

In the present work, we have studied the PAT proteins in the LBs of one type of inflammatory cell, the mast cell (MC). Mast cells derive from progenitor cells that leave the bone marrow, circulate in the bloodstream, and home in to virtually all vascularized tissues (19). There, the progenitor cells differentiate into mature MCs, with stem cell factor (SCF) being the major local factor responsible for the differentiation process (20). Comprehensive electron microscopic studies of MCs in various tissues have revealed that LBs are found particularly in human lung (3) and gut MCs (21), and sometimes in skin MCs (22).

A significant observation by Dvorak et al. was that LBs in MCs serve as storage sites for arachidonic acid (AA), a finding that implicated these organelles in eicosanoid biosynthesis in MCs (3). Since then, surprisingly little knowledge has been gained about the lipid composition of MC lipid bodies, and no information is available about which, if any, of the various PAT family members they contain. Fortunately, several protocols for the generation of human MCs have been established (23), rendering it possible to perform detailed studies on formation, structure, and function of LBs in these cells. We have recently defined culture conditions to generate mature and functional human MCs of the connective tissue type from peripheral blood-derived $CD34^+$ progenitors in the presence of SCF (24). In the present work, we found that differentiation of such $CD34^+$ progenitor cells into mature MCs invariably associates with a steady increase in the number and size of LBs. Treatment of MCs with unsaturated fatty acids accelerated the formation of LBs, and exogenously added arachidonic acid was efficiently incorporated into triacylglycerols, the predominant lipid class in the bodies. PLIN2 and PLIN3 were expressed in the developing and mature MCs, the former member being localized to the surface of LBs, and the latter being distributed throughout the cytoplasm in a punctate pattern. The demonstration of the genesis in cultured human MCs of arachidonate-enriched, PAT protein-containing LBs opens new avenues for detailed mechanistic studies of the specific functions of LBs in the pathobiology of these inflammatory cells.

MATERIALS AND METHODS

Cell culture

Mature human MCs were generated exactly as described previously (24). Briefly, $CD34^+$ progenitor cells were obtained from fresh buffy coats prepared from peripheral blood of healthy blood donors (Finnish Red Cross Blood Transfusion Service, Helsinki, Finland). The buffy coats were suspended in PBS, layered over Ficoll-Paque (1.77 g/l) (GE Healthcare), and the interface containing mononuclear cells was harvested after centrifugation. $CD34^+$ progenitor cells were enriched by positive immunomagnetic selection using MACS affinity columns (Milteny, Biotec). The isolated $CD34^+$ cells were cultured at 37°C under serum-free conditions in Iscove's Modified Dulbecco's Medium (IMDM) supplemented with BIT 9500 serum substitute (StemCell Technologies), L-glutamine (2 mM), 2-mercaptoethanol (0.1 mM), penicillin (100 U/ml) and streptomycin (100 μg/ml), human recombinant SCF (100 ng/ml), and different human recombinant cytokines (all from PeproTech, Rocky Hill, NJ). The human MC line LAD2, originally established from a MC sarcoma (25), was cultured at 37°C under serum-free conditions in IMDM containing BIT 9500 serum substitute, L-glutamine (2 mM), 2-mercaptoethanol (0.1 mM), penicillin (100 U/ml), streptomycin (100 μg/ml), and human recombinant SCF (100 ng/ml).

Oil Red O staining of cells

Mast cells were sedimented (*Cytospin*, Shandon Instruments) onto glass slides (15×10^3 cells/slide) and fixed with 10% neutral buffered formalin solution (Sigma). The cells were then stained with Oil Red O for 30 min and counterstained with Mayer's hematoxylin. Coverslips were mounted with aqueous medium to retain Oil Red O staining (Aquamount, DAKO). Images were captured with a Nikon Eclipse E600 microscope (original magnification, 40×).

Flow cytometry

Lipid bodies in cultured MCs were quantified by flow cytometry. For this purpose, the MCs were first probed with monoclonal anti-human c-kit antibody [allophycocyanin (APC)-conjugated mouse anti-human CD117, 4 μg/ml, BD Pharmingen] for 20 min, after which the cells were incubated with the fluorescent dye BODIPY 493/503 (10 μg/ml, Molecular Probes) for 10 min to stain intracellular LBs. Subsequently, the cells were washed, resuspended in PBS, and analyzed (1×10^4 cells/measurement) using a LSR II flow cytometer (BD Pharmingen). To quantify LBs in MCs after exocytosis of their cytoplasmic secretory granules (degranulation), the MCs were first passively sensitized in the presence of human IgE (1 μg/ml, DiaTec), and then triggered to degranulate by incubating them in the presence of polyclonal rabbit anti-human IgE (1 μg/ml, Millipore) for 1 h. Finally, the degranulated MCs were fixed with 4% paraformaldehyde in PBS (pH 7.4) for 15 min at room temperature, washed, and resuspended in FACS buffer (PBS containing 0.5% BSA and 0.025% NaN_3). For staining of intracellular organelles, the cells were permeabilized by incubation in FACS buffer containing 1% saponin for 20 min at room temperature. The permeabilized cells were then incubated with primary antibodies (mouse anti-human MC tryptase, 10 μg/ml, ABD Serotec; or APC-conjugated mouse IgG1 κ Isotype Control, BD Pharmingen) for 75 min at 4°C, washed, and probed with secondary antibody [phycoerythrin (PE)-conjugated goat anti-mouse IgG, 2 μg/ml, BD Pharmingen]. Prior to FACS analysis, the cells were stained with BODIPY 493/503 (10 μg/ml) for 10 min at room temperature. Unstimulated MCs served as controls and were analyzed exactly as described for the activated MCs.

Incubation of mast cells with fatty acids

Fatty acid:BSA complexes were prepared as follows. Stock solutions of a fatty acid sodium salt (stearate, Sigma, S3381; oleate, Sigma, O7501; or arachidonate, Sigma, A8798) were combined with a stock solution of fatty acid-free BSA (Sigma, A6003) at a

molar ratio of 6:1 (fatty acid:BSA) under nitrogen at 37°C for 15 min. All stock solutions were prepared in LDL buffer (150 mM NaCl, 0.24 mM EDTA, pH 7.4). Mast cells were incubated separately with the various fatty acid:BSA complexes (final fatty acid concentration, 400 μM) at 37°C for 18 h. In some experiments, the cells were incubated with fatty acid:BSA complexes in the presence of the long-chain acyl-CoA synthetase inhibitor Triascin C (5 μM, Enzo) or its vehicle (0.1% DMSO). After the incubations, the cells were washed twice with PBS before further analysis.

RT-PCR

Total RNA was isolated from cultured human MCs and LAD2 cells (RNeasy kit, QIAGEN), and cDNA was generated by RT-PCR (M-MLV reverse transcriptase, Promega). Human tissue mix cDNA (Clontech) was used as a positive control. For RT-PCR, specific oligonucleotide primers were designed for *plin1* (5′-CTT TAA CCA AAC TTG TGG CC-3′ and 5′-TAC TCA GAA AGT GAC ACT AG-3′), *plin2* (5′-AGT GGA AAA GGA GCA TTG GA-3′ and 5′-GTC TCC TGG CTG CTC TTG TC-3′), *plin3* (5′-GCT ACT TCG TAC GTC TGG GGC-3′ and 5′-TTT CTC AGT GAT TCC AGG GG-3′), *plin4* (5′-CCA AAG ACC TGG TGT GTT CC-3′ and 5′-AGC ACA GCC TTG GAG GTT T-3′), and *plin5* (5′-GTG GCC AGC AGT GTC ACG GG-3′ and 5′-GGA GCC GAG GCG CAC AAA GT-3′). Beta-actin primers (5′-AGA GCC TCG CCT TTG CCG AT-3′ and 5′-CAC CAT CAC GCC CTG GTG C-3′) were used as internal positive controls. All PCR products were T/A-cloned into pCR2.1-TOPO vector (Invitrogen) and confirmed by DNA sequencing using standard sequencing primers M13F and M13R.

Immunoblotting

For the preparation of total cell lysates, the MCs derived from $CD34^+$ progenitor cells and the LAD2 MCs were washed twice with PBS, lysed in RIPA buffer (50 mM Tris-HCl, 150 mM NaCl, 2 mM EDTA, 1.1% NP40, 0.1% SDS, pH 8.0) containing complete protease inhibitor cocktail (Roche), and incubated on ice for 1 h. The proteins in the lysate were separated by SDS-PAGE under reducing conditions, and then transferred onto a nitrocellulose membrane (Hybond-C Extra; Amersham Biosciences). Nonspecific binding sites were blocked by incubating the membrane with 5% nonfat dry milk in 1× TBS-T buffer (150 mM NaCl, 10 mM Tris, 0.1% Tween 20, pH 8) for 1 h at room temperature. Immunodetection was performed using guinea pig anti-human adipophilin (antiserum 1:1000, GP41, Progen Biotechnik) or guinea pig anti-human TIP47 (antiserum 1:5000, GP30, Progen Biotechnik) followed by incubation with HRP-labeled rabbit anti-guinea pig IgG (1:10 000, Invitrogen). The signals were detected using an enhanced chemiluminescence method (Pierce).

Confocal immunofluorescence microscopy

Cytospin preparations of MC suspensions were fixed with 4% paraformaldehyde and 0.025% glutaraldehyde for 20 min. Nonspecific binding sites were blocked with 3% goat serum containing 0.1% saponin and 0.2 M glycine in PBS (pH 7.4). The mast cells were then incubated with primary antibodies (guinea pig anti-human TIP47, 1:500, GP30, Progen; or mouse anti-human adipophilin, 16 ng/ml, AP125, Progen) in 3% goat serum containing 0.1% saponin in PBS (pH 7.4) for 2 h at room temperature. After incubation, the cells were washed and probed with secondary antibodies (Alexa Fluor-594 goat-anti guinea pig IgG or Alexa Fluor-594 goat anti-mouse IgG, 4 ng/ml each; Molecular Probes) for 1 h at room temperature. Lipid bodies were visualized using BODIPY 493/503 (10 μg/ml), and nuclei were counterstained with DAPI (4',6-diamidino-2-phenylindole). The samples were mounted in fluorescence mounting medium (DAKO), and z-stacks were captured with a 63× Plan Apo NA 1.40 lens of a LSM 5 DUO confocal laser scanning microscope (Zeiss).

Transmission electron microscopy

Mast cells were fixed with 2% glutaraldehyde in 0.1 M Na-cacodylate buffer (pH 7.4) for 2 h at room temperature, and then pelleted by low-speed centrifugation, resuspended in 0.1 M Na-cacodylate buffer, and embedded in 2% low-melting agarose (Sigma, A9045). Briefly, the standard transmission electron microscopy (TEM) processing involved postfixation with 1% osmium tetroxide, after which the samples were dehydrated through a graded series of ethanol and acetone, and gradually embedded in Epon. After polymerization at 60°C for 16 h, thin sections were cut and mounted on copper grids and stained with uranyl acetate and lead citrate. The stained sections were viewed at 80 kV with a Tecnai 12 transmission electron microscope (EM Unit, Institute of Biotechnology, University of Helsinki) using a 1k × 1k Gatan Multiscan 794 CCD camera. Montages (3k × 3k) were collected using the Gatan montage software.

Isolation of lipid bodies

Lipid bodies were isolated as described by Prattes et al. (26). Briefly, MCs were collected by centrifugation (300 *g*), washed with PBS, and gently resuspended with H_2O for cell lysis. The lysates were layered onto 250 mM sucrose, 50 mM Tris, pH 7.4, 25 mM KCl, and 5 mM $MgCl_2$, and centrifuged at 70,000 *g* at 4°C for 1 h. The LBs floated to the top fraction, which was collected and used for further analyses.

Thin-layer chromatography

Lipids were extracted from isolated LBs according to the method of Bligh and Dyer (27). Solvents were evaporated under nitrogen, and the lipids were dissolved in chloroform:methanol (2:1; v/v). Various lipid classes were separated by thin-layer chromatography (TLC) on HPTLC Silica gel 60 (Merck, Germany). Hexane:diethylether:acetic acid:H_2O (26:6:0.4:0.1; v/v) and chloroform:methanol:acetic acid:H_2O (10:3:1.6:0.7; v/v) were used as solvents for neutral lipids and phospholipids, respectively. The separated lipids were visualized by exposing the Silica gels to 3% $CuSO_4$ and 8% H_3PO_4 and subsequent heating at 160°C. Appropriate lipid standards were purchased from Sigma.

Mass spectrometry

Mast cells were incubated with arachidonate:BSA complexes (molar ratio 6:1; final arachidonate concentration, 400 μM), and the LBs were isolated as described above. Subsequently, the lipids of the LBs were extracted according to Folch et al. (28). After evaporation under constant nitrogen flow, the extracted lipids were dissolved in chloroform:methanol (1:2, v/v) containing 4% aqueous NH_3 (25% solution added just prior to analysis) for direct infusion experiments (flow rate 7 μl/min) using a Quattro Micro triple-quadrupole electrospray ionization mass spectrometer (Micromass, Manchester, UK). The instrument was used to detect positive ions either in the single-stage or in tandem MS mode. A fingerprinting method detecting neutral losses of AA and of other fatty acids from TG $(M+NH_4)^+$ ions was applied (29). Nitrogen was used as the nebulizer (500 l/h) at 130°C, and argon was used as the cone gas (40 l/h). The source temperature was set to 80°C. The cone, extractor, and RF lens potentials were set at 50 V, 2 V, and 0.3 V, respectively. A voltage of 3.8 kV was set for the capillary. The spectra were scanned from *m/z* 300 to *m/z* 1,100 with a frequency of 1 scan/4 s. The data were analyzed using the MassLynx 4.0 software (Waters).

RESULTS

To generate mature and functional mast cells, human peripheral blood-derived $CD34^+$ progenitor cells obtained from 18 different donors were cultured under serum-free conditions for up to 15 weeks (24). To analyze whether intracellular neutral lipid storage sites are formed during the maturation process, the MCs were stained with Oil Red O (**Fig. 1**). Six weeks after initiation of the cultures, only occasional small Oil Red O-positive LBs were identified in the MCs (Fig. 1A). At week 9, when the cultures consisted of a homogenous population of cells with the phenotype of mature human connective tissue-type MCs [i.e., when all cells contained tryptase- and chymase-containing cytoplasmic granules (not shown)], the number of the LBs had dramatically increased (Fig. 1B). The Oil Red O-positive cytoplasmic LBs also gained in size, as can be seen when comparing the MCs at 12 weeks (Fig. 1C) and 15 weeks (Fig. 1D) of culture. Each of the 18 cell populations was heterogeneous in terms of the number and size of the cytoplasmic LBs at any given time point of culture. Thus, some cells contained many large LBs, whereas other cells contained a variable number of small bodies or were even totally devoid of them. However, on average, a steady time-dependent increase in the number and size of LBs in all 18 cell cultures was observed, thus rendering each cell population progressively more homogenous in terms of its neutral lipid content.

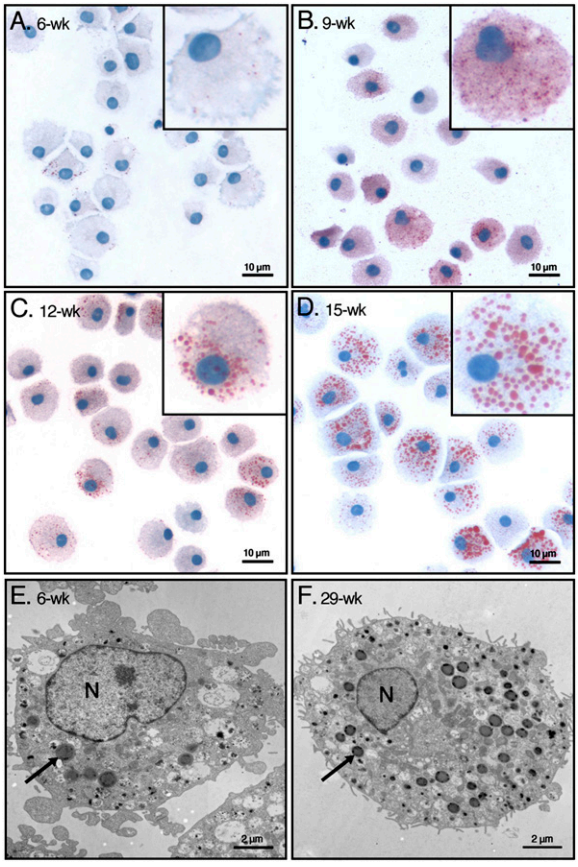

Fig. 1. Identification of LBs in human MCs with light and with electron microscopy. Human peripheral blood-derived $CD34^+$ progenitor cells from 18 donors were grown under defined culture conditions, which induced their differentiation into mature MCs, as described in *Materials and Methods*. A–D: The cells were stained with Oil Red O/hematoxylin at the indicated weeks in culture. Representative images of cells from a single donor are shown. Each inset shows one typical cell representative for the corresponding time point in culture. E, F: Mast cells from an early (6-week) and late (29-week) culture were analyzed by transmission electron microscopy. In each panel, one typical LB is indicated with an arrow. N, nucleus; wk, week.

More detailed information on the ultrastructural morphology and distribution of MC lipid bodies in the cytoplasm was obtained by transmission electron microscopy (TEM). This method allowed us to identify LBs as discrete organelles at both early and later stages of maturation (Fig. 1E, F). As previously described by Dvorak et al. (30), the LBs were clearly visible in the cytoplasm as electron-dense round structures, whereas the nucleus and other cytoplasmic compartments were less electron dense. To obtain quantitative insight into the time-dependent increase of number and size of MC lipid bodies, we analyzed the dynamics of this process by flow cytometry. The neutral lipids in the LBs were stained with the fluorescent dye BODIPY 493/503. As shown in **Fig. 2**, over a period of at least 11 weeks, fluorescence intensities in cultured MCs derived from three different donors (A, B, and C) increased continuously and with only small differences. Overall, the findings demonstrate that cytoplasmic LBs are formed in human peripheral blood-derived $CD34^+$ progenitor cells when the cells are induced to mature into MCs under the well-defined cell culture conditions used here. For all following experiments, only mature MCs (14 weeks or older) were used.

To gain information on the fate of LBs upon MC activation with ensuing exocytosis of the cytoplasmic secretory granules, we compared resting MCs with those having

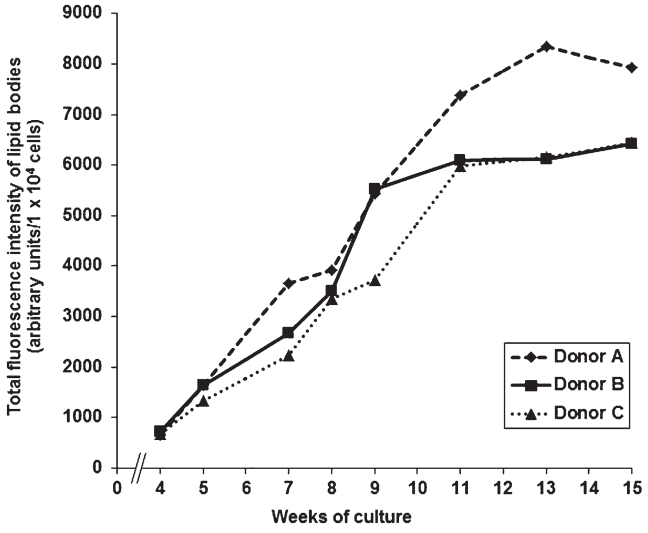

Fig. 2. Quantification of LBs in maturing MCs. The cumulative volumes of LBs in 10,000 MCs each derived from three different MC donors were analyzed by flow cytometry as a function of culture time. The results of each donor (A, B, and C) are shown as fluorescence intensities. The number of weeks of culture is indicated.

undergone degranulation (**Fig. 3**). For this purpose, MCs were immunologically activated by antigen-induced IgE cross-linking to trigger their degranulation. After 1 h of stimulation, no visible changes in the localization or morphological appearance of intracellular LBs were observed (Fig. 3A, B). Magnifications of representative LBs and secretory granules of resting and activated MCs are shown in Fig. 3C. The morphological appearance of the LBs remained unaltered, whereas the electron density of the membrane-bound granules became reduced, reflecting loss of granule components into the incubation medium space. To gain quantitative insight into the exocytotic process, we analyzed the total intracellular complement of LBs in resting versus degranulated MCs by flow cytometry (Fig. 3D). The extent of MC degranulation was estimated by determining the cellular content of the granule protease tryptase before and after stimulation, and the LB content was assessed by BODIPY 493/503 fluorescence. One hour after the immunological stimulation, no significant reduction in BODIPY 493/503 mean fluorescence intensity was observed in the stimulated cells. In sharp contrast, the activated MCs showed a 40% reduction in the mean immunofluorescence intensity of tryptase, thereby demonstrating degranulation with an accompanying loss of their tryptase content. Taken together, the results confirm that cytoplasmic LBs are granule-independent organelles, which are not cosecreted with the granules upon MC activation.

Next, we studied the presence of LB surface proteins of the PAT family in the $CD34^+$-derived MCs and in LAD2 MCs by RT-PCR using sequence-specific primers. The LAD2 cell line, a well-studied human MC analog, can be stimulated to degranulate in an IgE-dependent manner (25). Strong expression of *plin2* and *plin4* and lower levels of expression of *plin1* and *plin3* were observed in $CD34^+$-derived MCs (**Fig. 4**, lane 1). *Plin5* transcript was not detected, even when tested under a variety of PCR conditions. For comparison, RT-PCR data showed that LAD2 cells also

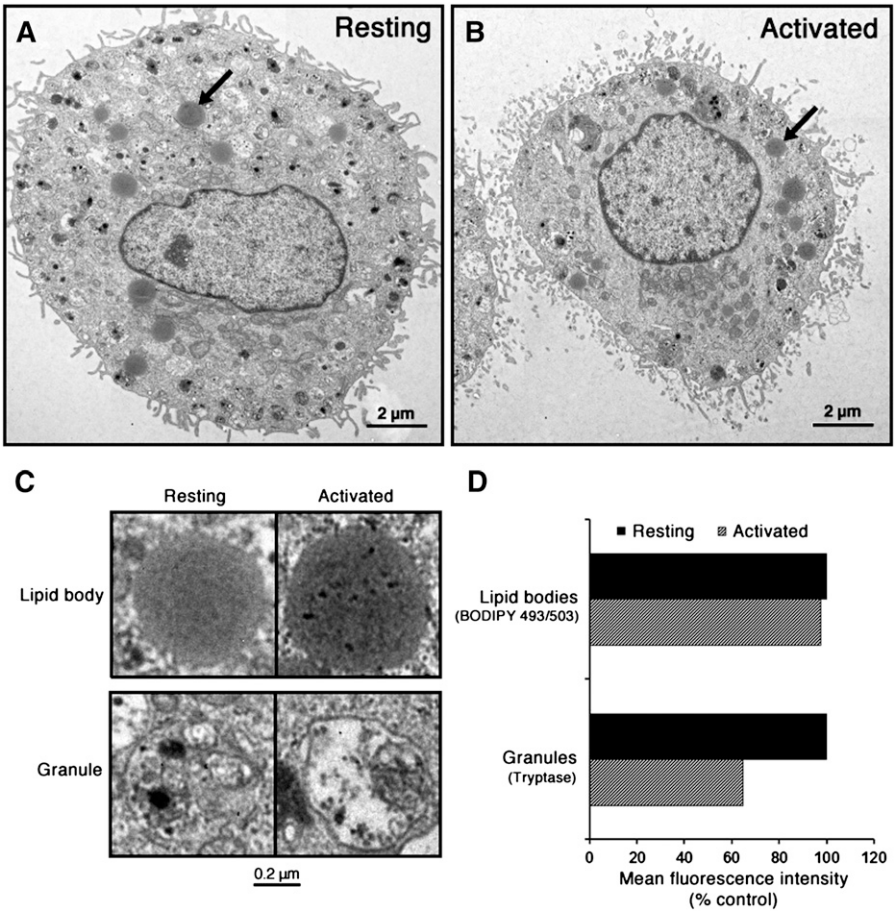

Fig. 3. Lipid bodies in resting and degranulated MCs. A, B: Mast cells from resting and immunologically activated cells (at 14 weeks of culture) were analyzed by transmission electron microscopy. In both panels, one typical LB is indicated with an arrow. C: Magnifications of typical LBs and secretory granules of resting and activated MCs. D: Mature MCs (at 16 week of culture) were activated for 1 h via IgE cross-linking to induce their degranulation (activated cells). Control cells were incubated in the absence of anti-IgE (resting cells). Then, all cells were fixed, permeabilized, and incubated with anti-tryptase antibody, washed, and probed with phycoerythrin-conjugated goat anti-mouse IgG. Cytoplasmic LBs were stained with fluorescent BODIPY 493/503, and the cells were analyzed by flow cytometry. The values shown are mean fluorescence intensities (1×10^4 cells/sample) for the stimulated cells expressed as percentages of fluorescence intensities of resting cells, and they represent the averages of values obtained with cells from two donors.

express *plin1*, *plin2*, *plin3*, and *plin4*, but not *plin5* (Fig. 4, lane 2). Thus, our data reveal for the first time that PAT genes are transcribed in human MCs. The presence of transcripts of these four genes (*plin1*, *plin2*, *plin3*, and *plin4*), and the absence of *plin5* was confirmed in MCs derived from each human donor studied (n = 8). We next tested for the presence of PLIN2 and PLIN3 proteins in total lysates of MCs and LAD2 cells by immunoblotting (**Fig. 5**). Using specific antibodies against PLIN2 and PLIN3, bands of the expected sizes (48 kDa and 47 kDa, respectively) were detected. In both types of MC, strong expression was obtained for PLIN2, whereas under our experimental conditions, PLIN3 appeared to be expressed at lower levels. Together, our data obtained by RT-PCR and immunoblotting revealed the presence in MCs of LB-associated proteins typically found in other types of LB-containing cells.

To obtain information about the intracellular localization of the two PLINs, LBs in $CD34^+$-derived MCs were stained with BODIPY 493/503 fluorescent dye, and the proteins were visualized by immunofluorescence microscopy (**Fig. 6**). Confocal slices through the MCs revealed the localization of PLIN2 solely in the circumference of LBs, whereas the cytoplasm failed to show any positive staining for this protein (Fig. 6A). In contrast, PLIN3 was diffusely distributed in the cytoplasm of the MCs in a punctate pattern and could hardly be found colocalized with the LBs (Fig. 6B). These differences were also clearly observed in the respective xz- and yz-planes.

For compositional analysis, LBs were isolated from MCs, and their lipids were extracted and separated by thin-layer chromatography (**Fig. 7**). As shown in Fig. 7A, the neutral lipid fraction was composed of TG, cholesteryl esters (CE), nonesterified fatty acids (NEFA), and unesterified cholesterol (UC). Triacylglycerols represented the most abundant neutral lipid class, whereas much smaller amounts of cholesterol esters, nonesterified fatty acids, and unesterified cholesterol were present in the LBs. An analysis of the glycerophospholipid fraction (Fig. 7B) revealed that the major phospholipid in the bodies is lyso-phosphatidylcholine (lyso-PC), with small amounts of phosphatidylcholine (PC) and sphingomyelin (SM) present. Similar results were obtained in isolated LBs from LAD2 cells (data not shown).

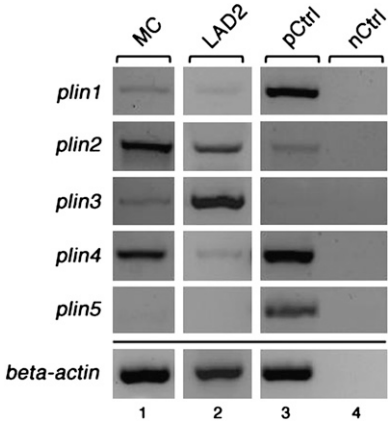

Fig. 4. Expression of PAT family members in human MCs. Transcript levels of the PAT family members *plin1, plin2, plin3, plin4,* and *plin5* were determined by RT-PCR using mRNA from human MCs at 14 wk of culture (MC, lane 1), LAD2 cells (LAD2, lane 2), and sets of sequence-specific primers. Human reference total RNA was used as positive control (pCtrl, lane 3), and PCR performed without the addition of template served as negative control (nCtrl, lane 4). Beta actin-specific primers were used to test the quality of cDNA templates (bottom panel). The PCR products were analyzed by agarose gel electrophoresis.

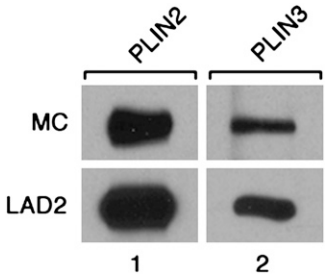

Fig. 5. PLIN2 and PLIN3 proteins in $CD34^+$-derived MCs and LAD2 MCs. Lysates of $CD34^+$-derived MCs (MC; 80 μg protein per lane) and LAD2 cells (LAD2; 70 μg protein per lane) were analyzed by Western blotting with guinea pig anti-human PLIN2 antiserum (lane 1) and with guinea pig anti-human PLIN3 antiserum (lane 2), respectively. Bound primary antibodies were visualized with HRP-labeled rabbit anti-guinea pig IgG.

Of particular interest was to learn whether LB formation can be induced by incubation of MCs with various fatty acids. For this purpose, MCs were incubated for 18 h with stearic acid (SA; 18:0), oleic acid (OA; 18:1), or AA (20:4), each complexed with BSA at a molar ratio of 6:1 (fatty acid:BSA), after which LBs were detected by Oil Red O staining. A clear increase in the number of LBs was observed in MCs incubated with OA or AA, but not with SA (images not shown). This finding prompted us to evaluate the quantitative changes in LB content of fatty acid-treated MCs. The cells were treated with SA, OA, or AA for 18 h, after which the LBs were quantified by flow cytometry (**Fig. 8**). When compared with control cells, no significant induction was observed after SA treatment, whereas the LB content was increased by 45% and 30% in OA- and AA-treated MCs, respectively. We also tested the effect of Triacsin C, a potent inhibitor of long-chain acyl-CoA synthetases 1, 3, and 4 (31) on the fatty acid-induced LB formation. No significant inhibition of LB growth was observed in MCs treated with SA. In contrast, lipid body growth was attenuated in OA- and AA-treated cells when Triacsin C was added to the incubation medium.

As for other inflammatory cells, the LBs in human lung MCs have been reported to incorporate arachidonic acid into their triacylglycerols (10). Therefore, we tested whether the cultured MCs are capable of esterifying arachidonic acid into the large triacylglycerol pool of their LBs. For this purpose, MCs were incubated with arachidonic acid for 18 h, after which LBs were isolated, and their lipids extracted and analyzed by tandem mass spectrometry (**Fig. 9**). The positive ion mass spectrum revealed that MC lipid bodies contain a mixture of phospholipids and neutral lipids, mainly TG. The TG species were typically

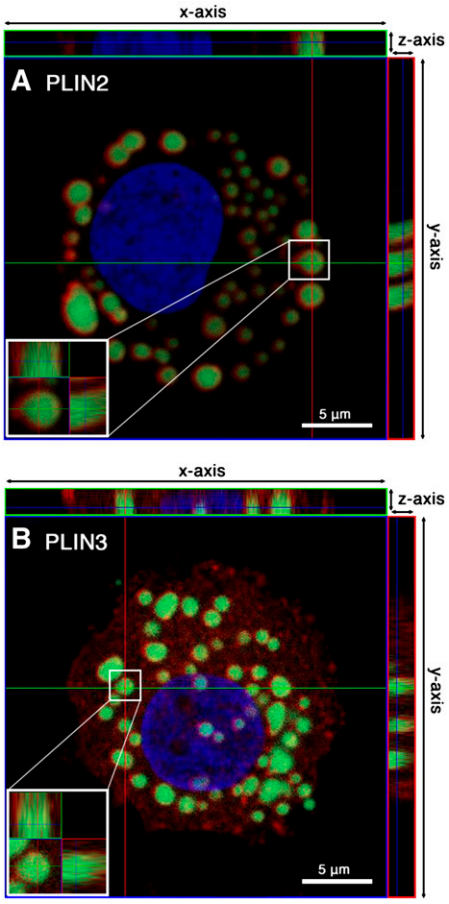

Fig. 6. Intracellular localization of PLIN2 and PLIN3 in MCs. For the analysis of the intracellular distribution of PLIN2 (A) and PLIN3 (B), MCs were probed with mouse anti-human PLIN2 or with guinea pig anti-human PLIN3. The primary antibodies were probed with Alexa Fluor-594 goat anti-mouse IgG (A) or Alexa Fluor-594 goat anti-guinea pig IgG (B). LBs were stained with BODIPY 493/503, and nuclei were counterstained with DAPI. Orthogonal projections of confocal z-stacks of representative LBs are shown (A, B). The main images of both panels show an xy-section of a MC at the z-positions indicated by dark blue lines in the xz-plane (x-axis/z-axis; small top rectangular figure) and the yz-plane (y-axis/z-axis; small right rectangular figure). Insets (A, B) show magnified orthogonal views of the indicated single LBs.

observed in the mass range *m/z* 900 to 1,050 (Fig. 9A). Scanning for the neutral loss of 321 Da specifically identified the exogenously applied arachidonic acid in the different triacylglycerol species (Fig. 9B). In fact, the most important AA-containing TG species contained two or three AA chains in the same molecule (see Fig. 9 legend). These results demonstrate definitively that mast cells can incorporate AA into their TG and suggest that the triacylglycerols in their lipid bodies may serve as a cytoplasmic storage pool for arachidonic acid.

DISCUSSION

This study focuses on the characterization of cytoplasmic lipid bodies in mast cells during their phenotypic maturation from $CD34^+$ progenitor cells derived from human

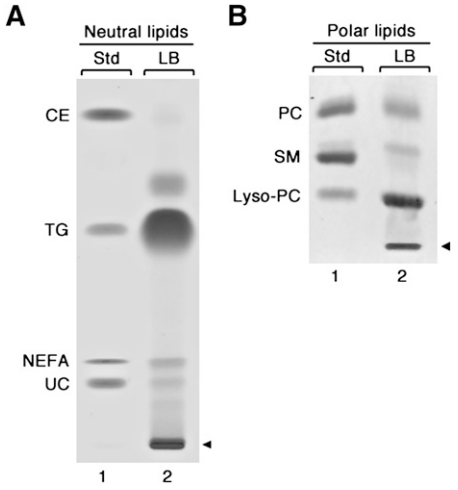

Fig. 7. Lipid composition of human MC lipid bodies. Lipid bodies were isolated from human MCs at 18 wk of culture, and their lipids were extracted and separated by thin-layer chromatography. A, B: Lane 1 contains the indicated lipid standards (Std), and lane 2 contains the lipids of the isolated LBs. A: Neutral lipids. B: Polar lipids. Arrowheads indicate site of sample application.

peripheral blood. As in other MC differentiation protocols (23) and, in fact, in human tissues in vivo, the development of MCs requires the continuous presence of stem cell factor. Therefore, determining the role, if any, of SCF on LB formation during mast cell maturation is precluded. In our protocol (24), the mature MCs produced are exclusively of the connective tissue-type [i.e., mast cells containing both tryptase and chymase (TC-MC)]. Thus, the results

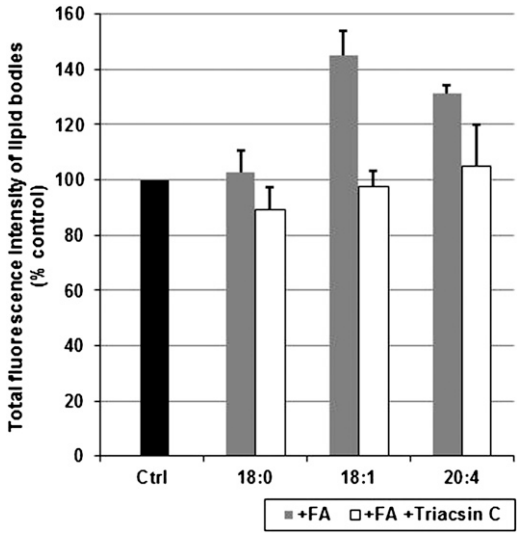

Fig. 8. Induction and inhibition of lipid body formation in MCs. Mast cells were incubated in the presence of stearic acid (18:0), oleic acid (18:1), or arachidonic acid (20:4), each complexed to BSA (molar ratio 6:1) in the absence or presence of the long chain acyl-CoA synthetase inhibitor Triacsin C at 37°C for 18 h. Lipid bodies were quantified by flow cytometry. Fluorescence intensities of the treated cells are shown and expressed as percentages of the fluorescence intensities of untreated control cells. Values represent the mean ± SD of cells (1×10^4 cells/sample) obtained from three donors (n = 3). Ctrl, control; FA, fatty acid.

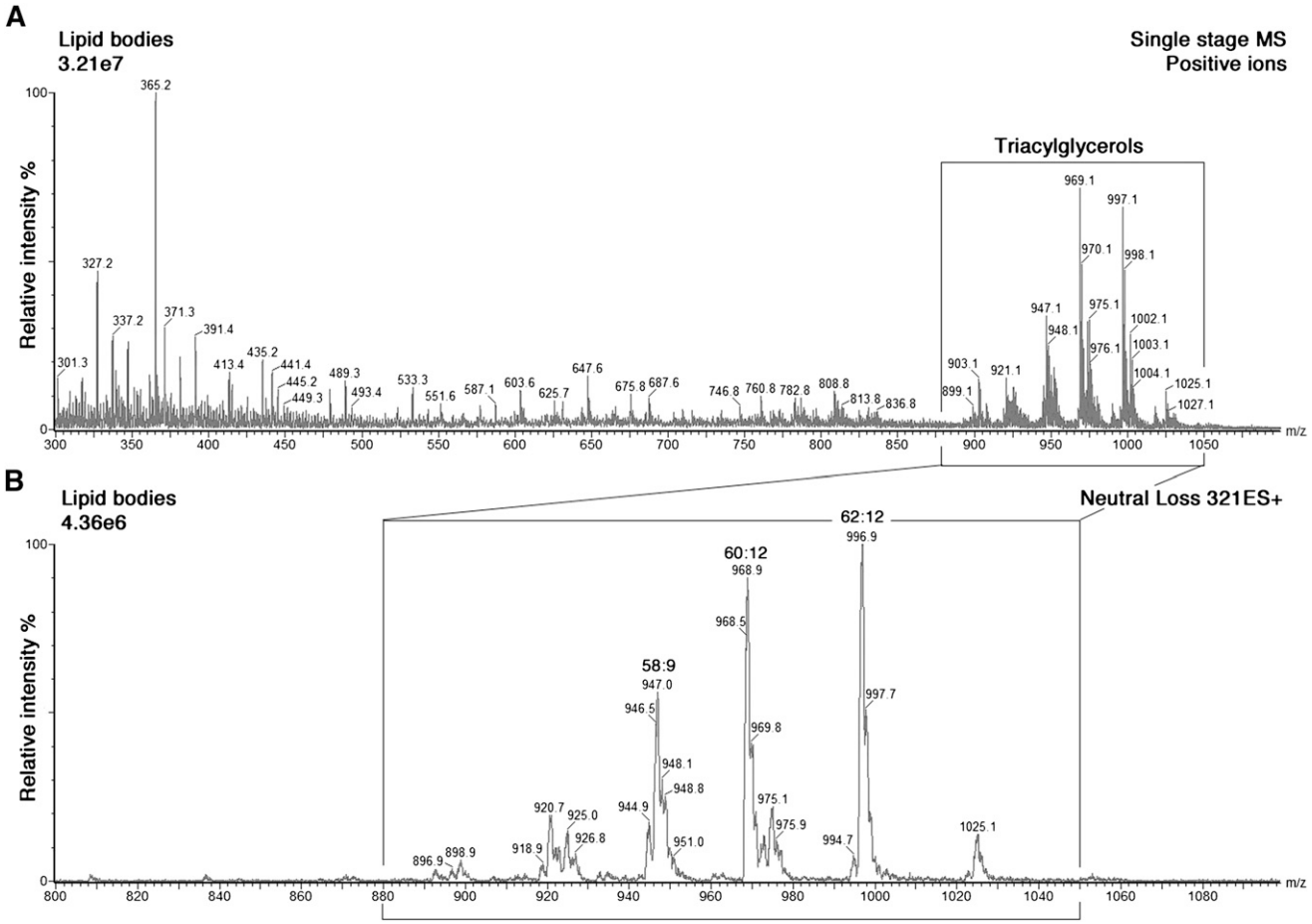

Fig. 9. Mass spectrometric analysis of MC lipid bodies. Lipid bodies were induced in MCs by incubating the cells in the presence of arachidonic acid, as described in Fig. 8. The bodies were then isolated, and their lipids extracted and analyzed by mass spectrometry. A: Positive ESI-MS of total lipid extract of LBs. Triacylglycerols (small rectangular box) are detected between *m/z* 880 and 1,050. B: Arachidonic acid-containing triacylglycerols (large rectangular box) were detected by the neutral loss scan for 321 amu during ESI-MS of neutral lipids extracted from LBs. The main arachidonic-acid-containing triacylglycerol species, denoted [sum of acyl carbons]:[sum of double bonds in the chains] with their *m/z* values and most likely acyl chain composition in parenthesis, were 58:9 (*m/z* 946; 18:1-20:4-20:4), 60:12 (*m/z* 968; 20:4-20:4-20:4) and 62:12 (*m/z* 996; 20:4-20:4-22:4). The intensity scales of the spectra were normalized to the largest signal in the selected *m/z* range. amu, atomic mass unit.

are obtained in a well-defined cell population representing one of the two major human mast cell types (32). Recently, human cord blood-derived mast cells have been reported to contain LBs after in vitro differentiation and cultivation in the presence of 10% fetal bovine serum (33). Here, the mast cells were differentiated in serum-free medium, which contained 1% (140 μM) fatty acid-containing BSA. Hence, the albumin-bound fatty acids were the only exogenous source of lipids in the differentiation medium. In accordance with albumin possessing two to three high-affinity and up to five intermediate-affinity binding sites for fatty acids (34), we measured a concentration of 700 μM fatty acids in the differentiation medium. This concentration is in the range of that in the extracellular fluids of the human body (i.e., in the physiological environment of MC differentiation in vivo). In any case, the total lipid concentration in the serum-free differentiation medium was lower than in standard cell culture media containing 10% serum. Based on these considerations, it is notable that the in vitro-differentiated mast cells generated LBs in a highly consistent fashion. This fact may indicate that, at least in part, mast cell LB formation requires cellular denovo lipid synthesis during maturation. The steady increase in total LB content in differentiating mast cells from all 18 donors supports the notion that LB formation is an innate property of TC-MC. However, comparison of mast cell cultures from different donors at a given period of maturation revealed small differences in both the average number and size of LBs (Fig. 2). Similarly, although all mast cell cultures were maintained under the same conditions, there were apparent minor donor-to-donor differences in the tendency to form cytoplasmic LBs (not shown). These qualitative differences may reflect functional heterogeneity of the LBs, an aspect that remains to be investigated. Inasmuch as all donors were healthy volunteers (samples provided by the Finnish Red Cross Blood Transfusion Service), such variation may also reflect genetic heterogeneity of the study population.

Regarding the implications of our observations during TC-MC differentiation for research on human mast cells in general, the following aspects of the phenotypic variation of MCs require consideration. TC-MCs are typically found in the skin, and they are widely distributed in most internal organs and tissues of the human body. Regarding mucosal surfaces of the body, note that in the gastrointestinal tract, the mucosal and submucosal layer predominantly contain T-MCs and TC-MCs, respectively. In contrast, in the bronchial tree of the lung, T-MCs predominate in both layers (32). Of great interest is a recent report of a phenotypic switch of bronchial T-MC in severe asthma that results in a greater proportion of TC-MC in the bronchial submucosa. The increase in the number of TC-MC was associated with an increased concentration of prostaglandin D2 (PGD2) in the bronchoalveolar lavage fluid. Since TC-MCs are known to produce more PGD2 than T-MC (35), the findings suggest that the excess of PGD2 originated in the TC-MC (i.e., the MC type studied in this work). In the atherosclerotic human coronary intima, the relative proportion of TC-MC of all mast cells ranges from 0% to 100% (36). However, which, if any, of the mast cells populating atherosclerotic lesions contain LBs is not known. In analogy to the mast cells in the lung, eicosanoid production in the MC present in the arterial wall may vary depending on the severity of the disease. It will be of major interest to determine whether the relative abundance of LBs in the different types of coronary mast cells correlate with clinical outcomes. Moreover, as the generation of eicosanoids is LB dependent (7), these and our above-described findings in diseased bronchial and coronary tissues support the value of in vitro-generated TC-MC as surrogates for the different populations of TC-MC obtained from tissue sites with different (patho)physiological microenvironments. The culture protocol for human TC-MC differentiation applied here should facilitate investigations of the roles of microenvironmental factors as they relate to the different local functions of mast cells, particularly the LB-dependent formation of lipid mediators (37).

Inasmuch as studies on the generation of LB-derived lipid mediators require a detailed characterization of the biology of the LBs in mast cells, we subjected MCs and their LBs to further analyses. Shown here for the first time, human MCs express several PAT proteins. This family of proteins is associated with LB metabolism in a variety of cell types (13). Analysis of the TC-MCs demonstrated the expression of *plin1*, *plin2*, *plin3*, and *plin4* at the transcriptional level. Among these, we selected for further analysis by immunofluorescence and immunoblotting the proteins PLIN2 and PLIN3, as they play major roles in the stabilization and formation of LBs in human macrophages, another type of inflammatory cell (38). In accordance with previous immunofluorescence studies on human macrophages (39), the images obtained by confocal microscopy identified PLIN2 adjacent to the LB surface (Fig. 6), whereas PLIN3 showed a diffuse distribution in the cytoplasm of mast cells. It remains to be ascertained by alternative methodologies whether PLIN3 can, under certain conditions, be associated with the surface of LBs. In any case, the molecular characterization of PAT family proteins provided unambiguous evidence for the LBs of TC-MCs being equivalent to those described in other types of inflammatory cells.

Ultrastructural studies have revealed that the major fraction of the cytoplasm of MCs is filled with secretory granules and that only a smaller part of the cytoplasm harbors LBs (30). The electron microscopic method used here was specifically aimed at the visualization of LBs and allowed us to distinguish them from cytoplasmic secretory granules (Figs. 1 and 3). The LBs could be recognized as electron-dense organelles of various sizes and increasing numbers during the differentiation of MCs. Importantly, the total volume of LBs, as determined by flow cytometry, and their ultrastructural morphology remained unaffected during mast cell activation and ensuing degranulation (Fig. 3). Taken together, our observations strongly support the previous conclusion by Dvorak et al. in lung MCs that LBs are not cosecreted with the cytoplasmic secretory granules upon degranulation (40). Thus, different methodologies applied to human MCs of different origin demonstrate that in these cells, LBs are indeed granule-independent organelles.

In the LBs of the developing and mature MCs, triacylglycerols were the most abundant class of lipids, whereas cholesteryl esters were present only in low amounts (Fig. 7). Thus, these LBs, like those of human lung MCs (10), appear to correspond to the lipid droplets of adipocytes rather than to those of macrophage foam cells. Although mature mast cells in various human tissues contain LBs (3, 21, 22), the factors leading to, or required for, the generation of these organelles in the various tissue environments are unknown. The in vitro system for MC maturation employed here may help to identify yet unknown players in the processes leading to LB formation in MCs. To date, the stimuli described for induction of LB genesis include LPS, cytokines, chemokines, and fatty acids (41). Similar to the observations in eosinophils, monocytes, and basophils (41), LB formation in MCs was found to be stimulated by the unsaturated fatty acids oleic acid and arachidonic acid, but not with the saturated fatty acid stearic acid (Fig. 8). Significantly, the stimulatory effect was diminished by coincubation with Triascin C, an inhibitor of long-chain acyl-CoA-synthetase (ACSL) 1, 3, and 4, the ACSL isoforms known to be localized to lipid droplets of murine adipocytes (31). Studies in progress are designed to determine whether any or all of these enzymes activate(s) certain fatty acids required for the formation of MC lipid bodies.

Research on inflammatory cell types has identified LBs as active sites for the conversion of arachidonic acid, released from different lipids by phospholipases, into eicosanoids (7). However, the mechanisms by which AA-containing TGs are formed and the AA mobilized under the influence of certain cellular stimuli remain to be defined. Interestingly, in the context of lipid mediator formation by MCs, early electron microscope studies in human lung MCs have revealed LBs as storage sites for

arachidonic acid, suggesting that these organelles contribute to eicosanoid biosynthesis and/or metabolism (3). Subsequent investigations demonstrated that a remarkable amount of arachidonic acid is associated with the large triacylglycerol pool of human lung MCs (10). Here, we show by tandem mass spectrometric analysis that the triacylglycerol fraction of isolated arachidonic acid-induced MC lipid bodies incorporates a large portion of the MC's total content of arachidonic acid. This implies that TC-MC lipid bodies can serve as reservoirs for arachidonic acid, a precursor of eicosanoid biosynthesis.

In conclusion, our current investigations demonstrate that human mast cells derived from $CD34^+$ progenitors in peripheral blood, which are MCs of the connective tissue type (i.e., surrogates of MCs intimately involved in the pathogenesis of allergic asthma, rheumatoid arthritis, and cardiovascular diseases), may be a new tool to study regulatory mechanisms in LBs, with particular emphasis on arachidonic acid metabolism, eicosanoid biosynthesis, and ensuing release of proinflammatory lipid mediators.

The authors thank the Biocenter Finland National Electron Microscopy Unit, Institute of Biotechnology, University of Helsinki, for providing facilities.

REFERENCES

1. Murphy, D. J. 2001. The biogenesis and functions of lipid bodies in animals, plants and microorganisms. *Prog. Lipid Res.* **40:** 325–438.
2. Gandotra, S., C. Le Dour, W. Bottomley, P. Cervera, P. Giral, Y. Reznik, G. Charpentier, M. Auclair, M. Delepine, I. Barroso, et al. 2011. Perilipin deficiency and autosomal dominant partial lipodystrophy. *N. Engl. J. Med.* **364:** 740–748.
3. Dvorak, A. M., H. F. Dvorak, S. P. Peters, E. S. Shulman, D. W. MacGlashan, Jr., K. Pyne, V. S. Harvey, S. J. Galli, and L. M. Lichtenstein. 1983. Lipid bodies: cytoplasmic organelles important to arachidonate metabolism in macrophages and mast cells. *J. Immunol.* **131:** 2965–2976.
4. Moreira, L. S., B. Piva, L. B. Gentile, F. P. Mesquita-Santos, H. D'Avila, C. M. Maya-Monteiro, P. T. Bozza, C. Bandeira-Melo, and B. L. Diaz. 2009. Cytosolic phospholipase A2-driven PGE2 synthesis within unsaturated fatty acids-induced lipid bodies of epithelial cells. *Biochim. Biophys. Acta.* **1791:** 156–165.
5. Weller, P. F., S. J. Ackerman, A. Nicholson-Weller, and A. M. Dvorak. 1989. Cytoplasmic lipid bodies of human neutrophilic leukocytes. *Am. J. Pathol.* **135:** 947–959.
6. Weller, P. F., R. A. Monahan-Earley, H. F. Dvorak, and A. M. Dvorak. 1991. Cytoplasmic lipid bodies of human eosinophils. Subcellular isolation and analysis of arachidonate incorporation. *Am. J. Pathol.* **138:** 141–148.
7. Bozza, P. T., I. Bakker-Abreu, R. A. Navarro-Xavier, and C. Bandeira-Melo. 2011. Lipid body function in eicosanoid synthesis: an update. *Prostaglandins Leukot. Essent. Fatty Acids.* Epub ahead of print. May 10, 2011; doi: .
8. D'Avila, H., C. M. Maya-Monteiro, and P. T. Bozza. 2008. Lipid bodies in innate immune response to bacterial and parasite infections. *Int. Immunopharmacol.* **8:** 1308–1315.
9. Paul, A., L. Chan, and P. E. Bickel. 2008. The PAT family of lipid droplet proteins in heart and vascular cells. *Curr. Hypertens. Rep.* **10:** 461–466.
10. Triggiani, M., A. Oriente, M. C. Seeds, D. A. Bass, G. Marone, and F. H. Chilton. 1995. Migration of human inflammatory cells into the lung results in the remodeling of arachidonic acid into a triglyceride pool. *J. Exp. Med.* **182:** 1181–1190.
11. Zehmer, J. K., Y. Huang, G. Peng, J. Pu, R. G. Anderson, and P. Liu. 2009. A role for lipid droplets in inter-membrane lipid traffic. *Proteomics.* **9:** 914–921.
12. Fujimoto, T., Y. Ohsaki, J. Cheng, M. Suzuki, and Y. Shinohara. 2008. Lipid droplets: a classic organelle with new outfits. *Histochem. Cell Biol.* **130:** 263–279.
13. Bickel, P. E., J. T. Tansey, and M. A. Welte. 2009. PAT proteins, an ancient family of lipid droplet proteins that regulate cellular lipid stores. *Biochim. Biophys. Acta.* **1791:** 419–440.
14. Lass, A., R. Zimmermann, M. Oberer, and R. Zechner. 2011. Lipolysis - a highly regulated multi-enzyme complex mediates the catabolism of cellular fat stores. *Prog. Lipid Res.* **50:** 14–27.
15. Larigauderie, G., C. Cuaz-Perolin, A. B. Younes, C. Furman, C. Lasselin, C. Copin, M. Jaye, J. C. Fruchart, and M. Rouis. 2006. Adipophilin increases triglyceride storage in human macrophages by stimulation of biosynthesis and inhibition of beta-oxidation. *FEBS J.* **273:** 3498–3510.
16. Wolins, N. E., B. K. Quaynor, J. R. Skinner, M. J. Schoenfish, A. Tzekov, and P. E. Bickel. 2005. S3–12, Adipophilin, and TIP47 package lipid in adipocytes. *J. Biol. Chem.* **280:** 19146–19155.
17. Wolins, N. E., J. R. Skinner, M. J. Schoenfish, A. Tzekov, K. G. Bensch, and P. E. Bickel. 2003. Adipocyte protein S3–12 coats nascent lipid droplets. *J. Biol. Chem.* **278:** 37713–37721.
18. Wang, H., M. Bell, U. Sreenevasan, H. Hu, J. Liu, K. Dalen, C. Londos, T. Yamaguchi, M. A. Rizzo, R. Coleman, et al. 2011. Unique regulation of adipose triglyceride lipase (ATGL) by perilipin 5, a lipid droplet-associated protein. *J. Biol. Chem.* **286:** 15707–15715.
19. Okayama, Y., and T. Kawakami. 2006. Development, migration, and survival of mast cells. *Immunol. Res.* **34:** 97–115.
20. Kitamura, Y., S. Go, and K. Hatanaka. 1978. Decrease of mast cells in W/Wv mice and their increase by bone marrow transplantation. *Blood.* **52:** 447–452.
21. Fox, C. C., A. M. Dvorak, S. P. Peters, A. Kagey-Sobotka, and L. M. Lichtenstein. 1985. Isolation and characterization of human intestinal mucosal mast cells. *J. Immunol.* **135:** 483–491.
22. Dvorak, A. M., and S. Kissell. 1991. Granule changes of human skin mast cells characteristic of piecemeal degranulation and associated with recovery during wound healing in situ. *J. Leukoc. Biol.* **49:** 197–210.
23. Andersen, H. B., M. Holm, T. E. Hetland, C. Dahl, S. Junker, P. O. Schiotz, and H. J. Hoffmann. 2008. Comparison of short term in vitro cultured human mast cells from different progenitors - peripheral blood-derived progenitors generate highly mature and functional mast cells. *J. Immunol. Methods.* **336:** 166–174.
24. Lappalainen, J., K. A. Lindstedt, and P. T. Kovanen. 2007. A protocol for generating high numbers of mature and functional human mast cells from peripheral blood. *Clin. Exp. Allergy.* **37:** 1404–1414.
25. Kirshenbaum, A. S., C. Akin, Y. Wu, M. Rottem, J. P. Goff, M. A. Beaven, V. K. Rao, and D. D. Metcalfe. 2003. Characterization of novel stem cell factor responsive human mast cell lines LAD 1 and 2 established from a patient with mast cell sarcoma/leukemia; activation following aggregation of FcepsilonRI or FcgammaRI. *Leuk. Res.* **27:** 677–682.
26. Prattes, S., G. Horl, A. Hammer, A. Blaschitz, W. F. Graier, W. Sattler, R. Zechner, and E. Steyrer. 2000. Intracellular distribution and mobilization of unesterified cholesterol in adipocytes: triglyceride droplets are surrounded by cholesterol-rich ER-like surface layer structures. *J. Cell Sci.* **113:** 2977–2989.
27. Bligh, E. G., and W. J. Dyer. 1959. A rapid method of total lipid extraction and purification. *Can. J. Biochem. Physiol.* **37:** 911–917.
28. Folch, J., M. Lees, and G. H. Sloane Stanley. 1957. A simple method for the isolation and purification of total lipides from animal tissues. *J. Biol. Chem.* **226:** 497–509.
29. Han, X., and R. W. Gross. 2001. Quantitative analysis and molecular species fingerprinting of triacylglyceride molecular species directly from lipid extracts of biological samples by electrospray ionization tandem mass spectrometry. *Anal. Biochem.* **295:** 88–100.
30. Dvorak, A. M. 2002. Ultrastructure of human mast cells. *Int. Arch. Allergy Immunol.* **127:** 100–105.
31. Soupene, E., and F. A. Kuypers. 2008. Mammalian long-chain acyl-CoA synthetases. *Exp. Biol. Med. (Maywood).* **233:** 507–521.
32. Irani, A. A., N. M. Schechter, S. S. Craig, G. DeBlois, and L. B. Schwartz. 1986. Two types of human mast cells that have distinct neutral protease compositions. *Proc. Natl. Acad. Sci. USA.* **83:** 4464–4468.
33. Minai-Fleminger, Y., M. Elishmereni, F. Vita, M. R. Soranzo, D. Mankuta, G. Zabucchi, and F. Levi-Schaffer. 2010. Ultrastructural evidence for human mast cell-eosinophil interactions in vitro. *Cell Tissue Res.* **341:** 405–415.
34. van der Vusse, G. J. 2009. Albumin as fatty acid transporter. *Drug Metab. Pharmacokinet.* **24:** 300–307.

35. Balzar, S., M. L. Fajt, S. A. Comhair, S. C. Erzurum, E. Bleecker, W. W. Busse, M. Castro, B. Gaston, E. Israel, L. B. Schwartz, et al. 2011. Mast cell phenotype, location, and activation in severe asthma: data from the severe asthma research program. *Am. J. Respir. Crit. Care Med.* **183:** 299–309.
36. Kovanen, P. T. 2007. Mast cells: multipotent local effector cells in atherothrombosis. *Immunol. Rev.* **217:** 105–122.
37. Shea-Donohue, T., J. Stiltz, A. Zhao, and L. Notari. 2010. Mast cells. *Curr. Gastroenterol. Rep.* **12:** 349–357.
38. Buers, I., O. Hofnagel, A. Ruebel, N. J. Severs, and H. Robenek. 2011. Lipid droplet associated proteins: an emerging role in atherogenesis. *Histol. Histopathol.* **26:** 631–642.
39. Robenek, H., S. Lorkowski, M. Schnoor, and D. Troyer. 2005. Spatial integration of TIP47 and adipophilin in macrophage lipid bodies. *J. Biol. Chem.* **280:** 5789–5794.
40. Dvorak, A. M., I. Hammel, E. S. Schulman, S. P. Peters, D. W. MacGlashan, Jr., R. P. Schleimer, H. H. Newball, K. Pyne, H. F. Dvorak, L. M. Lichtenstein, et al. 1984. Differences in the behavior of cytoplasmic granules and lipid bodies during human lung mast cell degranulation. *J. Cell Biol.* **99:** 1678–1687.
41. Melo, R. C., H. D'Avila, H. C. Wan, P. T. Bozza, A. M. Dvorak, and P. F. Weller. 2011. Lipid bodies in inflammatory cells: structure, function, and current imaging techniques. *J. Histochem. Cytochem.* **59:** 540–556.